Journal of Applied Mechanics and Technical Physics, Vol. 42, No. 3, pp. 529–532, 2001

EFFECT OF SHOCK-WAVE LOADING ON THE PROPERTIES OF CRYOGENIC TiNi — A SHAPE-MEMORY ALLOY

V. A. Ogorodnikov, N. N. Popov, I. V. Sevryugin, N. D. Sevryugina, V. I. Luchinin, S. V. Erunov, and O. A. Esin

UDC 539.37, 669.018.2

Results of an experimental study of the shock-wave deformation of TiNi and its effect on the crystallographic structure and temperature of austenite-martensite transformations are given. It is found that, for pressures of up to 2 GPa*, shock-wave loading changes the defect structure and parameters of the lattice; however, this does not lead to a noticeable change in the temperature of the austenite-martensite transformation and the manifestation of the shape-memory effect.*

Owing to their unique properties, alloys with the shape-memory effect (SME) are finding wide application in the industry and medicine [1–3]. In some cases, SME alloys can be used in the production of structural members subjected to shock-wave loading during operation [4]. With this fact in view, it is of interest to study the effect of shock-wave loading on the SME of these alloys. The information on this subject available in the literature, for example, for high-temperature alloys, is incomplete and contradictory. Bogdanov, Pikus, and Luchenok [5] found that shock loading leads to an increase in the temperatures of martensite transformations in a TiNi alloy. However, Likhachev and Shimanskii [6] did not observe this effect for the same TiNi alloy and at the same parameters of high-rate loading. An information on the effect of shock loads on the behavior of a cryogenic TiNi alloy is lacking in the literature.

In the present paper, we give results of an experimental study of the shock-wave deformation of a cryogenic TiNi alloy in the austenite state. With the use of specimens from this alloy, we study the effect of preliminary shock-wave loading of various intensities on the crystallographic structure and temperature of austenite-martensite transformations.

Shock-Wave Deformation of TiNi Alloys. To study the dynamic behavior of TiNi and the effect of pressure pulses on the crystallographic structure and its properties, we performed a series of tests at various intensities of shock-wave loading. The tests were performed on a ballistic shock complex [7] with the use of alloys characterized by the following mass fractions: 51.4% Ti, 45.8% Ni, and 2.8% Fe (alloy 1) and 50.7% Ti, 46.1% Ni, and 3.2% Fe (alloy 2).

A specimen of diameter 28 mm and height 20 mm was pressed in a steel case with an outer diameter of 90 mm. This target was loaded by a steel impactor of diameter 75 mm and height 22 mm and then it was decelerated in a low-density medium (polyethylene chip). In each test, the velocity of the free surface of the specimen $W(t)$ was recorded by a capacitive sensor of diameter 20 mm with a safety ring [8]. The approach velocity of the impactor W_0 and the shock-wave velocity in the specimen D were measured by means of electrical contacts. Using the profile $W(t)$, we estimated the dynamic yield point $\sigma_s = 0.5[(1-2\nu)]/(1-\nu)]\rho_0 D_1 W_1$, where ν is Poisson's ratio, ρ_0 is the density of a TiNi alloy, D_1 is the velocity of the elastic wave, and W_1 is the velocity of the free surface of the specimen at the moment the elastic wave arrives at it.

Figure 1 shows the profiles $W(t)$ obtained in the tests with alloys 1 and 2 at various velocities of the impactor W_0. Using curve 4, we show the free-surface velocity at the peak pressure W_*, and the velocities of the free surface for the elastic (W_1) and plastic (W_2) waves. One can see from Fig. 1 that, for the loading regimes considered, the TiNi alloy acts as an elastoviscoplastic body. A considerable dispersion of the compressive wavefront, which decreases with increase in the intensity of loading, is observed.

Institute of Experimental Physics, Sarov 607190. Translated from Prikladnaya Mekhanika i Tekhnicheskaya Fizika, Vol. 42, No. 3, pp. 175–179, May–June, 2001. Original article submitted July 18, 2000.

0021-8944/01/4203-0529 $25.00

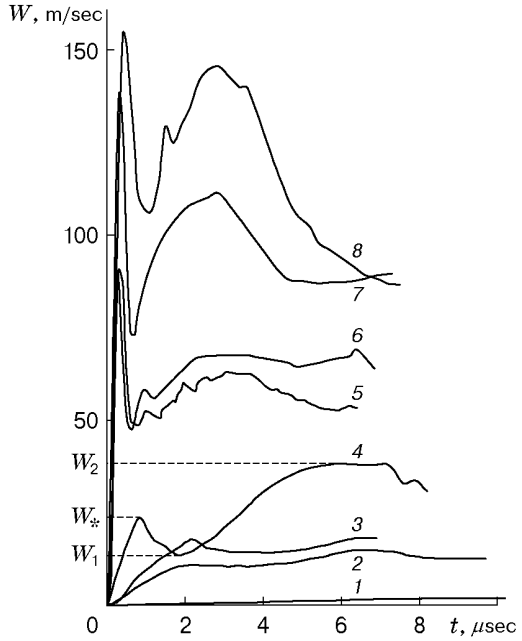

Fig. 1. Profiles of the free-surface velocity of alloys 1 and 2 for W_0 = 3.7 (1), 14.5 (2), 18.5 (3), 26.7 (4), 91.4 (5), 95.8 (6), 135.1 (7), and 150.8 m/sec (8).

TABLE 1

Test No.	Alloy	W_0, m/sec	u_*, m/sec	p_*, GPa	u_1, m/sec	p_1, GPa	σ_s, GPa	u_2, m/sec	D_2, km/sec	p_2, GPa
1	1	3.7	—	—	1.0	0.03	—	—	—	—
2	1	14.5	—	—	5.0	0.16	0.10	7.4	2.48	0.20
3	1	18.5	8.8	0.29	7.0	0.23	0.13	9.0	2.53	0.26
4	2	26.7	11.8	0.38	7.0	0.23	0.13	19.0	3.50	0.49
5	1	91.4	45.0	1.48	—	—	—	31.0	4.27	0.86
6	2	95.8	46.0	1.49	—	—	—	35.0	4.40	0.99
7	2	135.1	70.0	2.26	—	—	—	56.0	4.44	1.58
8	1	150.8	77.0	2.49	—	—	—	73.0	4.38	2.01

A two-wave configuration determined by the elastic-plastic transition occurs at $W_0 \geqslant 14.5$ m/sec, and the time interval between the fronts of the free-surface velocity for elastic (W_1) and plastic (W_2) waves decreases with increase in the intensity of loading. For $W_0 \geqslant 91.4$ m/sec, the elastic wave cannot be determined in an explicit form. In this case, the nonstationary behavior determined by the peak pressure in the elastic wavefront W_* becomes pronounced at $W_0 \geqslant 18.5$ m/sec. This peak pressure is similar to the sharp yield point, which is typical of certain metals in static and shock tests. A similar complex structure of the shock wave with a sharp yield point was observed, for example, for steel [9].

It should be noted that the profiles $W(t)$ measured with the use of specimens from different batches are almost identical at close velocities of the impactor (Test Nos. 5 and 6). Table 1 lists the peak-pressure parameters $u_* = W_*/2$ and p_*, the elastic-wave parameters $u_1 = W_1/2$, p_1, and σ_s, and the plastic-wave parameters $u_2 = W_2/2$, D_2, and p_2. In calculations by the formulas $p_* = \rho_0 c u_*$ and $p_1 = \rho_0 c u_1$, we used the values $\rho_0 = 6.3$ g/cm^3 and $D_* = D_1 \approx c = 5.2$ km/sec, and in the calculation by the formula $p_2 = p_1 + \rho_0(D_2 - u_1)(u_2 - u_1)$, we used the value of D_2 determined from the time interval from the moment of collision between the impactor and the specimen (electrocontact sensor) to the moment the plastic wave arrives at the free surface of the specimen (capacitive sensor). Figure 2 shows a section of the shock adiabat plotted with the use of the results obtained in tests with alloy 1.

Effect of Shock-Wave Loading of TiNi on the Crystallographic Structure, the Temperature of Austenite–Martensite Transformations, and the SME. After shock-wave loading, specimens of alloy 1 were cut into pieces along the loading direction. From these pieces, the samples of diameter 3 mm and height 10 mm with threaded ends were prepared. For x-ray phase measurements, the samples were chamfered by 2 mm. The

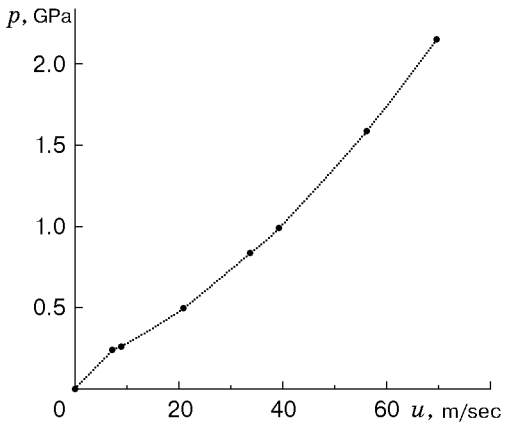

Fig. 2

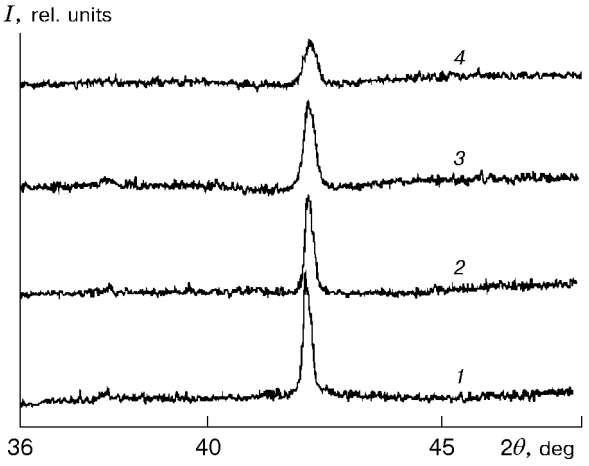

Fig. 3

Fig. 2. Shock adiabat of TiNi.

Fig. 3. Diffraction pattern of TiNi specimens in the austenite state for $W_0 = 3.7$ (1), 18.5 (2), 91.4 (3), and 150.8 m/sec (4).

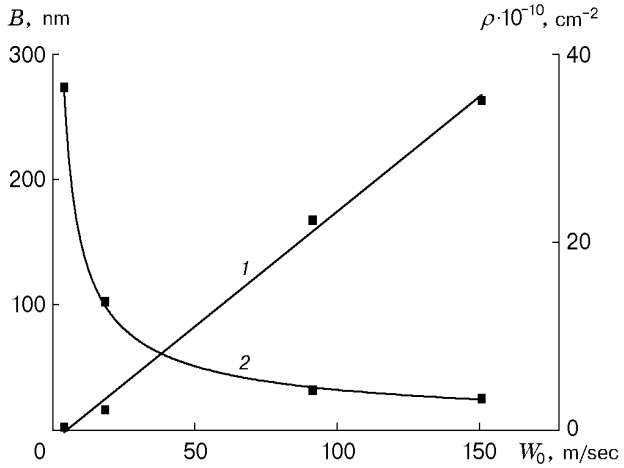

Fig. 4. Parameters of the defect structure in a TiNi alloy versus the intensity of shock-wave loading: curves 1 and 2 refer to ρ and B, respectively.

prepared samples and the samples-witnesses from the initial material were used to study the dislocation density, the grain sizes or the coherent-scattering region, the initial (A_{ini} and M_{ini}) and final (A_{fin} and M_{fin}) temperatures of the austenite and martensite transformations, respectively, by the x-ray structural method.

Figure 3 shows the diffraction patterns $I(2\theta)$ of the samples made of alloy 1 in the austenite state at $T = 293$ K and at impactor velocities ranging from 3.7 to 150.8 m/sec. One can see that the defect structure and parameters of the austenite lattice change with increase in the loading rate. Moreover, the width of the reflection line corresponding to the crystallographic plane (110) increases, whereas its intensity decreases. Using x-ray structural analysis results, we determined the parameters of the fine structure and the dislocation density [10].

Figure 4 shows the dislocation density ρ and the dimension of the coherent-scattering region B as functions of the loading rate W_0. These dependences show the noticeable evolution of the defect structure as the intensity of loading increases.

Table 2 gives dependences of the temperatures of the austenite (A_{ini} and A_{fin}) and martensite (M_{ini}) transformations on the loading rate which were determined in [11] by the x-ray diffraction method. Moreover, the temperatures of the reverse martensite transformation A_{ini} and A_{fin} were determined from the results of mechanical tests. The difference between the values of A_{ini} and A_{fin} obtained by different methods was within the experimental error.

TABLE 2

W_0, m/sec	A_{ini}, K	A_{fin}, K	M_{ini}, K
0	191 (194)	223 (208)	133
3.7	191	218	128
18.5	193	218	128
91.4	193 (186)	216 (207)	113
150.8	193 (187)	205 (204)	93

Note. The bracketed values of A_{ini} and A_{fin} refer to the reverse martensite transformation.

An analysis of the data given above shows that the temperature at which the direct martensite transformation begins M_{ini} decreases as the loading rate increases; it decreases by 40 K for the maximum impactor velocity 150.8 m/sec. This points to stabilization of the austenite phase. At the same time, the temperatures of the reverse martensite transformation A_{ini} and A_{fin} depend only slightly on the shock-wave intensity in the range of pressures considered, which is responsible for the increase in the width of the hysteresis of the martensite transformation in alloy 1. It is likely that this change in the temperature behavior is caused by the evolution of the defect structure in a TiNi alloy determined by the increase in the intensity of shock-wave loading.

It has been found that the shock-wave deformation of TiNi alloys 1 and 2 in the austenite state is complex. For alloy 1, a change in the defect structure and parameters of the austenite lattice is observed at pressures of up to 2 GPa; however, this does not lead to a considerable change in the temperatures A_{ini} and A_{fin} and the manifestation of the SME.

REFERENCES

1. J. Perkins, "TiNi and TiNi-x shape memory alloys," *Metall*, **3**, 153–163 (1981).
2. V. É. Gyunter, V. V. Kotenko, V. K. Polenichkin, and V. I. Itin, "The use of shape-memory alloys in medicine," *Izv. Vyssh. Uchebn. Zaved., Fiz.*, No. 5, 127–132 (1985).
3. D. D. Harrison and D. E. Hogson, *The Use of TiNi Alloys in Mechanical and Electrical Connections. The Shape-Memory Effect in Alloys* [Russian translation], Metallurgiya, Moscow (1979).
4. A. T. Razov and A. G. Chernyavskii, "The use of shape-memory alloys in space technology," in: *Modern Problems of Strength*, Proc. of XXXV Seminar (Pskov, September 15–18, 1999), Izd. Pskov. Politekh. Inst., Pskov (1999), pp. 254–259.
5. A. P. Bogdanov, I. M. Pikus, and A. P. Luchenok, "Effect of shock-wave loading on the structural factors of a TiNi compound," in: *Effect of High Pressures on Material Properties* [in Russian], Proc. of V Rep. Seminar (Kiev, August 8–12, 1983), Naukova Dumka, Kiev (1983), pp. 188–190.
6. V. A. Likhachev and S. R. Shimanskii, "Effect of the deformation rate on the reversible shape memory of TiNi," *Probl. Prochnosti*, No. 2, 65–68 (1988).
7. V. N. Mineev, V. P. Pogorelov, A. G. Ivanov, et al., "Setup for investigation of the behavior of materials and structures under dynamic loading," *Fiz. Goreniya Vzryva*, **14**, No. 3, 129–133 (1978).
8. A. G. Ivanov and S. A. Novikov, "Capacitive-sensor method for recording the instantaneous velocity of a moving surface," *Prib. Tekh. Éxp.*, No. 1, 135–139 (1963).
9. A. G. Ivanov, S. A. Novikov, and V. A. Sinitsyn, "Investigation of elastoplastic waves in iron and steel under explosive loading," *Fiz. Goreniya Vzryva*, **5**, 269–278 (1963).
10. S. S. Gorelik, Yu. A. Skakov, and L. N. Rastorguev, *Radiographic and Electron-Optic Analyses* [in Russian], Moscow Inst. of Steels and Alloys, Moscow (1994).
11. N. N. Popov, N. D. Sevryugina, M. Yu. Sidorkin, and I. V. Sevryugin, "Temperature measurement of the martensite–austenite transformation of a TiNi-based alloy by the x-ray phase method," *Fiz. Met. Metalloved.*, **86**, 137–144 (1998).